# Thermal conduction of carbon nanotubes using molecular dynamics

Zhenhua Yao[*] and Jian-Sheng Wang[†]

*Singapore-MIT Alliance, National University of Singapore, Singapore 117576*

Baowen Li

*Department of Physics, National University of Singapore, Singapore 119260*

Gui-Rong Liu

*Department of Mechanical Engineering,*

*National University of Singapore, Singapore 119260*

(Dated: February 2, 2008)

## Abstract

The heat flux autocorrelation functions of carbon nanotubes (CNTs) with different radius and lengths is calculated using equilibrium molecular dynamics. The thermal conductance of CNTs is also calculated using the Green-Kubo relation from the linear response theory. By pointing out the ambiguity in the cross section definition of single wall CNTs, we use the thermal conductance instead of conductivity in calculations and discussions. We find that the thermal conductance of CNTs diverges with the CNT length. After the analysis of vibrational density of states, it can be concluded that more low frequency vibration modes exist in longer CNTs, and they effectively contribute to the divergence of thermal conductance.

PACS numbers: 61.48.+c, 63.22.+m, 66.70.+f, 68.70.+w

## I.   INTRODUCTION

The carbon nanotube (CNT) was discovered by S. Iijima in 1991[1]. Since then, its unique mechanical, electrical and optical properties initiated intensive research on this quasi one-dimensional material[2]. CNTs have high Young modulus and strength[3], as well as high thermal conductivity. Many novel applications in various areas have been proposed, including nanoscale electronic devices in the next generation electronic technologies.

As the dimensions of electronic devices shrink to nanoscale, the thermal conduction problem becomes more and more important, as a significant energy may be dissipated in a compact space. However, it is very difficult to measure the thermal conducting ability of nanoscale devices. Furthermore, Fourier Law, which describes the macroscopic thermal conduction phenomena, may not be appropriate for low dimensional systems. Therefore, it is important to study the thermal conduction of nanoscale systems and to develop theoretical and computational methods for predicting the thermal properties of nanoscale materials and devices.

There are mainly two approaches to theoretically study the thermal conduction phenomena of nanoscale materials, the first is a macroscopic method using continuum models and kinetic theories, such as Boltzmann transport equation[4,5], the second is a fundamental microscopic method based on first principle atomistic simulations or quantum mechanical models. In the second approach, various methods are proposed to model the physical system and calculate the thermal conductivity. These methods include equilibrium and non-equilibrium molecular dynamics (MD) simulation as well as model-coupling theory, etc[6]. These methods model the physical system from scratch and make no empirical assumption.

The understanding of heat conduction and development of a complete theory is a long-standing and formidably difficult task. For insulating crystals, the problem of heat transportation by lattice vibrations is still far from be solved from some points of view. For mathematical simplicity, one-dimensional or two-dimensional lattices of atoms are naturally considered[6]. This issue has been addressed for several decades. Recently, Baowen Li *et al* established a connection between anomalous heat conduction and anomalous diffusion in one-dimensional systems[7], and Jian-Sheng Wang *et al* studied the anomalous thermal conduction in 1D chains by using MD and mode-coupling theory[8].

In CNTs generally two physical mechanisms contribute to the thermal conduction:

1. Electron–phonon interactions, which mainly depend on electronic band structures of and the electron scattering process, etc.

2. Phonon–phonon interactions, which depend on the vibrational modes of the lattice.

For semiconductor CNTs in room temperature, phonon–phonon interactions dominate the overall thermal conductivity, and electron–phonon interactions have only a small contribution due to the large band gap and low density of free charge carriers[9]. Fortunately this part contribution to thermal conduction can be well studied by using classical MD.

The phonon mean free path in the axial direction of CNTs is estimated to be very long, about 100 nm — $1\mu$m, and much longer than that of other materials as well as the size of simulation domain, thus the thermal conductivity of CNTs which are shorter than a few $\mu$m may have ballistic transport features[10]. On the other hand, the finite size effect constrains the phonon motion and causes the thermal conductance seems variable with the CNT length. Actually, it is difficult to make the simulation domain larger than phonon mean free path even on supercomputers, thus finding the "correct" value of thermal conductance remains a difficult task.

In the last few years, there are many research activities on this subject. Berber *et al* studied the thermal conductivity $\kappa$ of CNTs and the dependence of $\kappa$ on temperature and suggested that $\kappa$ is about 6600 W/mK for CNT (10,10) at room temperature[11]. J. Che *et al* calculated the thermal conductivity of diamond materials and CNTs, and showed that the theoretical value of thermal conductivity converges as the simulation system size increases. However, in their papers the errors of thermal conductivity values are too large to draw an accurate conclusion[12]. S. Maruyama *et al* studied the heat conduction in finite length CNTs using non-equilibrium MD and calculated the thermal conductivity from the measured temperature gradients and energy budgets in phantom molecules, and claimed that thermal conductivity of CNT $(5,5)$ diverges as the power law where the power index is $0.32$[10]. M. A. Osman *et al* calculated the temperature dependence of the thermal conductivity and found that $\kappa$ shows a peaking behavior before falling off at higher temperatures due to the onset of Umklapp scattering[13]. S. G. Volz investigated the thermal conductivity of bulk silicon crystals based on MD simulation using Stillinger–Weber potential, and found that $\kappa$ is independent to the length $L_x$ of nanowire when $L_x$ is larger than 16 lattice constants and the cross section area is smaller than a certain value[14].

In addition to these theoretical research there are some experimental work on the heat conduction of CNTs. D. Yang *et al* investigated the thermal conductivity of multi-wall CNTs using a pulsed photo-thermal reflectance technique, and suggested that the effective $\kappa$ could be about 200 W/mK[15]. P. Kim and L. Shi *et al* measured the thermal conductivity of single CNT using a microfabricated suspended device and found that $\kappa > 3000$ W/mK at room temperature[16]. J. Hone *et al* measured the temperature-dependent thermal conductivity of crystalline ropes of single-wall CNTs and argued that $\kappa$ is dominated by phonons at all temperatures[17].

In this work we use the Green–Kubo relation derived from linear response theory to examine the thermal conductance by calculating the heat flux autocorrelation functions. However, finite size artifacts are still involved due to the frequency cutoff and the artificial autocorrelation introduced by periodic boundary conditions, which is consistent with the results of S. Volz[14]. We find that the lowest frequency of lattice vibration modes is limited by the size of simulation domain, and the thermal conductance of an infinite long CNT maybe infinite.

## II.   COMPUTATION OF THERMAL CONDUCTIVITY USING MD

### A.   Green-Kubo relation and heat flux

In macroscopic model of thermal conduction, the thermal conductivity is defined from Fourier's law which is for heat flow under non-uniform temperature distribution. And the heat flux $\mathbf{j}$ can be defined as $\mathbf{j} = -\kappa \nabla T$, where $\kappa$ is the thermal conductivity tensor and $T$ is the temperature distribution.

From the intuition of Fourier's law, a simple approach to study the thermal conduction of CNTs is putting the two ends in two heat reservoirs with different temperature (usually $T_0 + \Delta T$ and $T_0 - \Delta T$, where $T_0$ is supposed to be the average temperature of the system), and measuring the heat flux along the axial direction and then calculating the thermal conductance. In simulations the heat flux should be collected after the system becomes steady, and a large number of averages over time are needed to get smooth temperature gradient curve and accurate heat flux data. However, the simulation domain which MD can efficiently handle is not large enough, and the temperature gradient due to reasonable tem-

4

perature difference of two heat reservoirs (please note that too small temperature difference gives large error and poor results) is far too large to be realistic. Moreover, as the thermal conductance strongly depends on the temperature, calculation results from non-uniform temperature distribution may not be accurate. P. Schelling *et al* systematically compared the equilibrium and non-equilibrium methods for computing the thermal conductivity of insulating materials[18] and mentioned these problems.

Due to aforementioned reasons, in this work we use the fluctuation–dissipation theorem from linear response theory which connects the energy dissipation to the thermal fluctuations in equilibrium state[5,19]. In this method, the thermal conductivity in axial direction of CNTs can be expressed in terms of heat flux autocorrelation function[5,19],

$$\kappa = \frac{1}{k_\mathrm{B}T^2V} \int_0^\infty \langle J(t)J(0)\rangle dt, \tag{1}$$

where $J(t) = \int \mathbf{j}(\mathbf{r},t)dV$ is the total heat flux in axial direction, and $V$ is the volume of the system. From the local energy balance equation

$$\frac{\partial \epsilon(\mathbf{r},t)}{\partial t} + \nabla \cdot \mathbf{j}(\mathbf{r},t) = 0, \tag{2}$$

where $\epsilon(\mathbf{r},t)$ is the energy density (i.e., energy per unit volume), and note that $\epsilon(\mathbf{r},t)$ and $\mathbf{j}(\mathbf{r},t)$ are macroscopic concepts, a microscopic expression for total heat flux can be derived as follows,

$$\mathbf{J}(t) = \frac{d}{dt} \sum_i \mathbf{r}_i(t)\epsilon_i(t), \tag{3}$$

where $\mathbf{r}_i(t)$ is the time-dependent coordinate of atom $i$. In MD simulation, the total potential energy can be divided among atoms, then the site energy $\epsilon_i(t)$ can be taken to be

$$\epsilon_i = \frac{1}{2}m_i\mathbf{v}^2 + \sum_j u(r_{ij}). \tag{4}$$

In the above equation, $u(r_{ij})$ is in fact a many-body potential[20], and the calculation of total heat flux $\mathbf{J}(t)$ is much more complicated in this case than in case of using a simple pairwise potential function.

## B.   Interatomic potential

Currently there are several choices of potential functions for describing interatomic interactions in carbon materials: Tersoff potential which was published in 1989 for the latest

parameters[20]; Brenner potential which was originally published in 1990[21] and revised in 2002[22]; Environment-Dependent Interaction Potential for carbon materials by N. A. Marks published in 2000[23]; and a new bond order potential which parameters are fitted to tight-binding results[24]. In these potentials, the latter two haven't been widely recognized, Brenner potential with latest parameters gives accurate results and is widely used. However, it is observed that in long-time micro-ensemble running[29], Brenner potential gives larger total energy deviation than Tersoff potential does due to its complicated interpolation functions. On the other hand, Tersoff potential is stable in long-time running according to our tests and gives fairly accurate results. Q. Zheng *et al* compared Tersoff and Brenner potentials in their theoretical analysis to the thermal conduction of single-wall CNTs[25] and got good results using both potentials, Berber has also used Tersoff potential to study the thermal properties of CNTs and calculated the thermal conductivity[11]. Therefore, in our simulation we use Tersoff potential.

In the past decades, Tersoff potential has been widely used to study the mechanical and thermodynamic properties of silicon and carbon materials, and results obtained are accurate and can be comparable to those from first principle methods, such as from tight-binding method and density functional theory. Tersoff potential can be formally written as a summation of pairwise interactions,

$$V_{\text{tot}} = \frac{1}{2} \sum_{ij} \left\{ f_{\text{c}}(r_{ij}) \left[ V_{\text{R}}(r_{ij}) - B_{ij} V_{\text{A}}(r_{ij}) \right] \right\}, \tag{5}$$

where $V_{\text{R}}$ and $V_{\text{A}}$ are the repulsive and attractive parts of the potential, and their functional forms are given below,

$$V_{\text{R}}(r) = A \exp(-\lambda r), \qquad V_{\text{A}}(r) = B \exp(-\mu r), \tag{6}$$

$$f_{\text{c}}(r) = \begin{cases} 1 & r < R \\ \frac{1}{2} \left[ 1 + \cos \frac{\pi(r-R)}{S-R} \right] & R \leq r \leq S \\ 0 & r > S \end{cases}, \tag{7}$$

where $f_{\text{c}}(r)$ is a cutoff function which explicitly restricts the interactions within the nearest neighbors, and dramatically reduces the redundant computation in the force/potential evaluation procedure. In Eq. (5) $B_{ij}$ is a bond order parameter and depends on the bonding

6

environment around atom $i$ and $j$. $B_{ij}$ implicitly contains multi-body information and thus the whole potential function is actually a multiple body potential. The function form of $B_{ij}$ can be written as follows,

$$B_{ij} = [1 + (\beta \zeta_{ij})^n]^{-\frac{1}{2n}} . \tag{8}$$

The detailed information and parameters of Eq. (5)~(8) are given in Tersoff's paper[20].

## C.  Finite size effect

One of major concerns in simulation of CNTs to calculate the thermal conductivity is the finite size effect due to periodic boundary condition applied in the axial direction. As the simulation is conducted in a periodic box, the long wavelength vibration mode of lattice is cut off while the CNT is short. This effect causes that a short CNT's thermal conductivity is smaller than a long CNT's. By using MD, we investigate the thermal conductivity of CNTs with different length as well as the relationship between the thermal conductivity and the length, to study its convergence with system size.

According to above discussions, a large system has more long wavelength vibration modes, and correspondingly has longer phonon mean free path. Thus for longer CNTs, the calculated thermal conductivity will be larger due of contribution of long wavelength vibration modes.

## D.  Thermal conductance vs thermal conductivity

It should be mentioned here that since an isolated single-wall CNT's cross section can be defined in different ways, its thermal conductivity has also arbitrary definitions and is not a well defined quantity. Some definitions of the cross section of single-wall CNT are:

1. Consider CNT as a solid cylinder, then the cross section area will be $\pi R^2$, where $R$ is the radius of CNT;

2. Consider CNT as a hollow cylinder, then the cross section area will be $2\pi R\delta$, where $\delta$ is the thickness of CNT shell. In literature usually two values of $\delta$ are used, one is 3.4 Å, which is the inter-layer distance of graphite materials, the other is 1.42 Å, which is the length of $sp^2$ bond.

Therefore, in literature many different values of thermal conductivity are reported, some of them mainly differ in the cross section definition.

Obviously, the definition of the cross section are is not important for the thermal conduction research of CNTs, as we only need to calculate and compare the results consistently. However, for comparing different results from different research groups, this arbitrary in the thermal conductivity calculation must be eliminated. In this work, we use the quantity of "thermal conductance", which equals to thermal conductivity times cross section area. Thus, the thermal conduction has the dimension of "Watt·meter/Kelvin".

### E.  Simulation procedure

In this work, CNTs with different size are investigated. Firstly, armchaired CNT $(10, 10)$ with different length are simulated, then CNT $(15, 15)$ and $(5, 5)$ are simulated. In our MD simulation program, time integration algorithm is implemented by using velocity Verlet method. For improving the computation performance, a new neighbor list algorithm using cell decomposition is employed[26]. In all simulation cases, periodic boundary condition is used only in the axial direction of CNTs. For each simulation case, we carry out the following three steps:

1. Firstly canonical ensemble MD is running for $10^5 \sim 5 \times 10^5$ steps in order to take the average system temperature to 300 K and wait until system reaches thermal equilibrium.

2. Then followed by micro-canonical ensemble running for another $10^5 \sim 5 \times 10^5$ steps and wait until system reaches a thermal equilibrium in new ensemble.

3. Finally micro-canonical ensemble MD continues to run and heat flux data are calculated and collected in every time step. After every $10^5$ steps, the power spectrum of heat flux data are online calculated, meanwhile, its arithmetic average and Fourier transform, which is heat flux autocorrelation function, as well as the statistical errors are calculated and dumped to disk files.

In this work, the last step runs infinitely and stops until accurate results are obtained after many times of average. Generally $10^8$ steps were carried out in this step, in other

words, about 1000 averages have been done to obtain the final data. Total amount of CPU time is about three months on 10 Pentium III 866MHz PCs and three dual-CPU Alpha EV67/667MHz workstations.

In MD simulation, time step is 0.8 fs, and the canonical ensemble simulation is implemented by using Nośe-Hoover algorithm[27].

## III.   RESULTS AND DISCUSSIONS

FIG. 1 shows the initial autocorrelation function of the total heat flux along the axial direction of CNT (10, 10) with 50, 100, 200 and 400 layers, and a very sharp decay in the beginning and following a very slow decay can be seen clearly. An oscillation in autocorrelation function can also be seen in the curves and it becomes larger when the CNT is longer. It can also been seen an increase of autocorrelation function values as the CNT length increases. The fast initial decay is believed to be contributed by high frequency vibrational modes in the CNT, and slow decay is contributed by low frequency modes which have much longer wavelength.
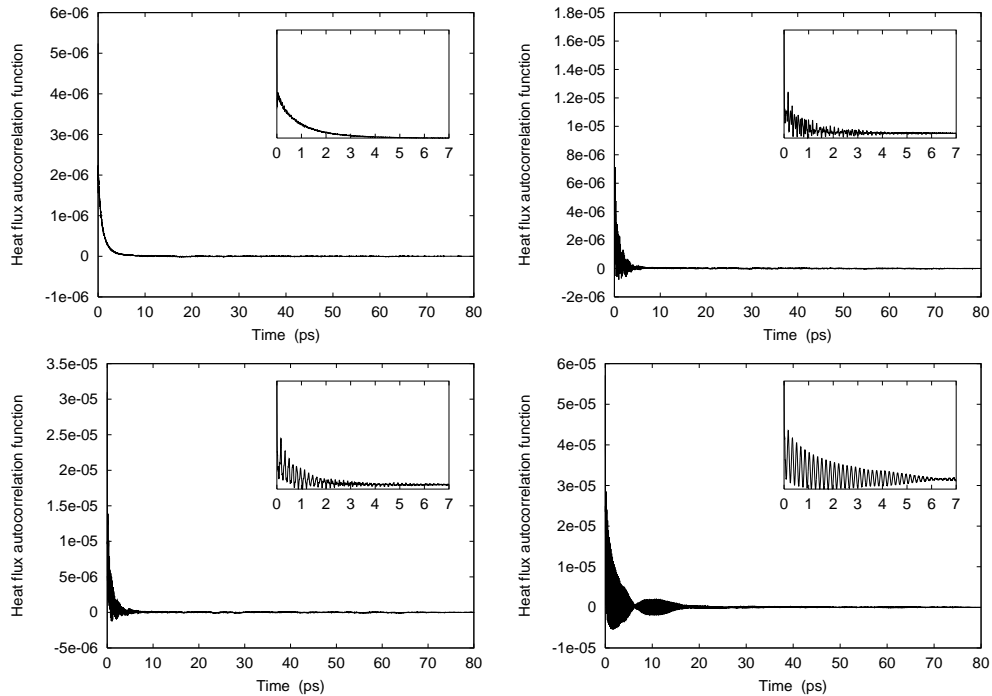


FIG. 1: Heat flux autocorrelation function of CNT (10, 10) with 50, 100, 200 and 400 layers, respectively (from left to right, top to bottom). Insets are initial decay in initial 8000 steps.

9

FIG. 2 is the log–log version of FIG. 1. Please note that data points in the range of 10000—100000 are in the order of $10^7 \sim 10^8$ and almost random errors. The origin of these errors are mainly due to inaccurate velocity trajectories and roundoff errors in floating operations. Data points in the range of 1—1000 correspond to initial decay in very early moment and the number of points is small (though this section seems quite long in the graph), thus the middle section in the range of 1000—10000 time step is most significant. and it can be seen that roughly the correlation function decays as power law $f(t) = ct^\alpha$.
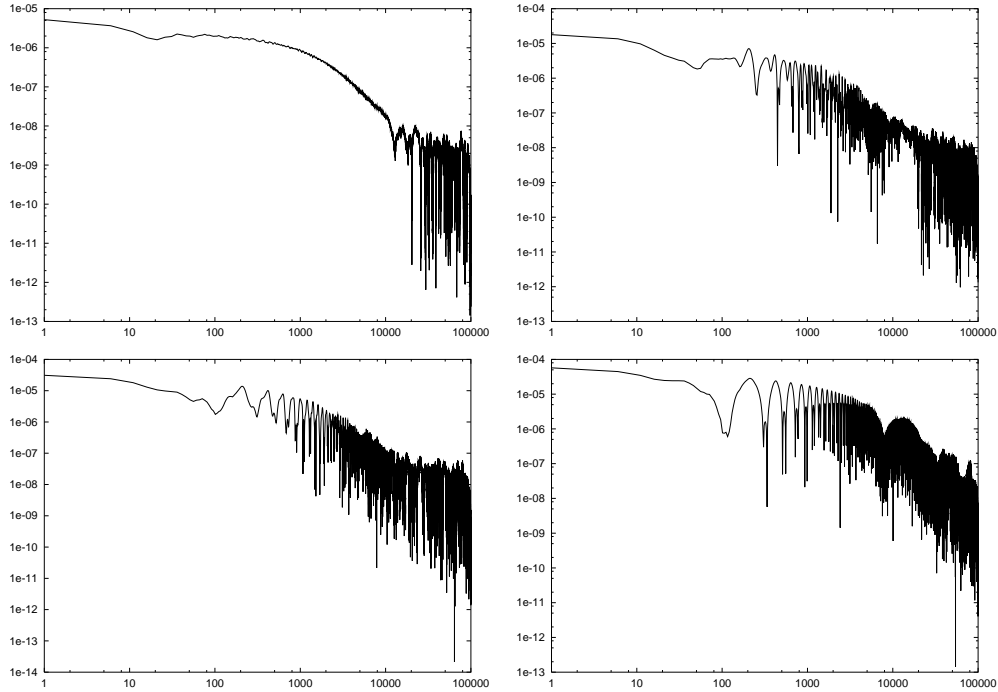


FIG. 2: Heat flux autocorrelation function (log-log) of CNT $(10, 10)$ with 50, 100, 200 and 400 layers, respectively (from left to right, top to bottom).

From data in FIG. 2 we calculate the power index $\alpha$ of heat flux autocorrelation function decay using linear interpolation method and showed the relationship between $\alpha$ and the length of CNT in FIG. 3. By using the mode-coupling theory, the knowledge of the asymptotic behavior of $\langle \mathbf{J}(t)\mathbf{J}(0)$ allows determining the dependence of thermal conductance on the system size $N^6$. From FIG. 3 it can been seen that the power index of heat flux autocorrelation function decay is about $-3/2$, and for certain cases it is near to $-1$, thus the thermal conductance $\kappa$ should converge to a finite value as the system size increases. However, when the length of CNTs is between $50 \sim 600$ layers in our work, there is no evidence that $\kappa$ will
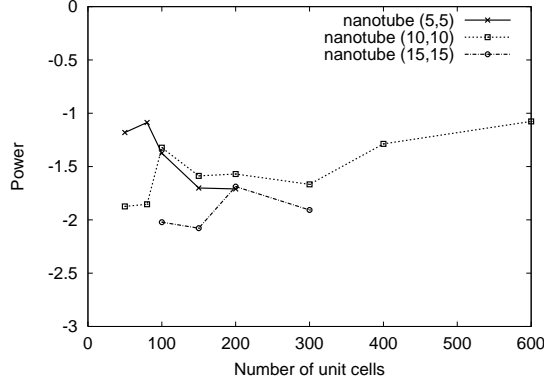
converge.



FIG. 3: Relationship between decay power index and length of CNT $(5,5)$, $(10,10)$ and $(15,15)$. (Power indices for shorter CNT have also smaller errors.)

Curves shown in FIG. 4 are the integration of heat flux autocorrelation function over time $t$. It can be seen that very slow decay doesn't contribute the thermal conductivity in a significant way, and initial fast decay due to long wavelength low frequency vibrational modes contributes mostly. Therefore, the cutoff of long wavelength vibrational modes will significantly influence the final result of thermal conductivity. Compared with CNT $(10,10)$, the integration of heat flux autocorrelation function for CNT $(5,5)$ converges hardly, especially for the longer CNTs. The integration of heat flux autocorrelation function for CNT $(15,15)$ is qualitatively the same as CNT $(10,10)$, and it converges fast, so we don't show it in FIG. 4.
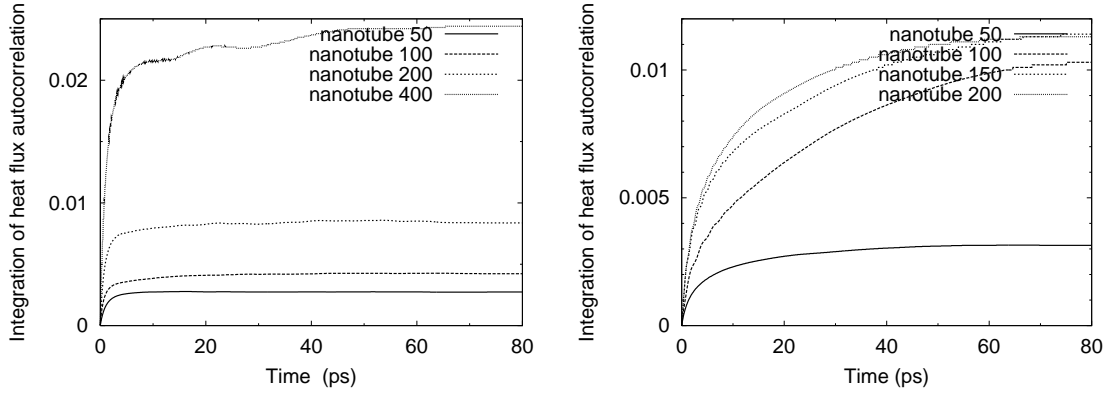


FIG. 4: Integration of heat flux autocorrelation function over time $t$ up to given number of time steps for CNT $(10,10)$ and $(5,5)$.

11

As the discussions in section II D, the absolute value of an isolated single-wall CNT is ambiguous because the cross section are is not well defined, so we discuss only thermal conductance. The relationship between the thermal conductance and the length of CNT is shown in FIG. 5. In all cases, the thermal conductance of single-wall CNT doesn't converge to a finite value as the increase of CNT length. In the figure we also give the standard errors of thermal conductance results and mark in the error bars. The error is calculated as follows,

1. In micro-canonical ensemble simulation, $N_{\text{tot}}$ number of time steps is carried out, thus $N_{\text{tot}}$ heat flux data points is collected.

2. Divide these heat flux data to $N$ groups, each group has $M$ heat flux data points, and calculate the heat flux autocorrelation function and integration for each group, respectively.

3. The final result is taken to be the average of $N$ groups of results in the second step. Meanwhile the standard error of the result is given by,

$$S_i = \sqrt{\frac{1}{N} \sum_{j=1}^{M} (\xi_j - \bar{\xi})^2}, \qquad i = 1, \cdots, N.$$
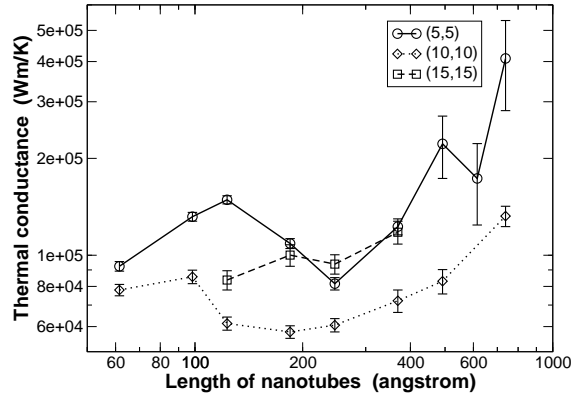


FIG. 5: Thermal conductance as a function of CNT length. In the graph solid line, dot line and dash line denotes the thermal conductance of CNT $(5,5)$, $(10,10)$, and $(15,15)$, respectively.

From FIG. 5 it can been seen that as long as the length of CNT increases, the thermal conductance increases correspondingly, and this trend has been discovered in literature[10]. If we consider the van der Waals thickness 3.4 Åas the thickness of CNT shell, and treat

CNT as a hollow cylinder, the thermal conductivity results are in good agreement with S. Maruyama's data[10].

In order to know why longer CNT has higher thermal conductance, we calculate the vibrational density of states (VDOS) by computing the power spectrum of velocity correlation function while the simulation is running, and the calculation can be expressed as follows[28],

$$D_z(\omega) = \int \exp(-i\omega t)\langle v_z(t)v_z(0)\rangle dt, \tag{9}$$

where $D_z(\omega)$ denotes the VDOS along the $z$ axis (i.e., the axial direction), $v_z(t)$ denotes the velocity of atoms in the $z$ axis. FIG. 6 shows the VDOS of CNTs with 50 and 100 layers, respectively. The inset of FIG. 6 shows the VDOS of two CNTs in full frequency range, and it seems that two curves are almost the same, this indicates that the middle and high frequency distribution of VDOS of two CNTs are roughly identical. However, from the graph of low frequency range, it can been seen that CNT with 100 layers has more low frequency vibration modes, this is why longer CNT has higher thermal conductance. We believe that why CNT with 100 layers has more low frequency modes is that it has larger simulation domain and then has longer phonon mean free path.
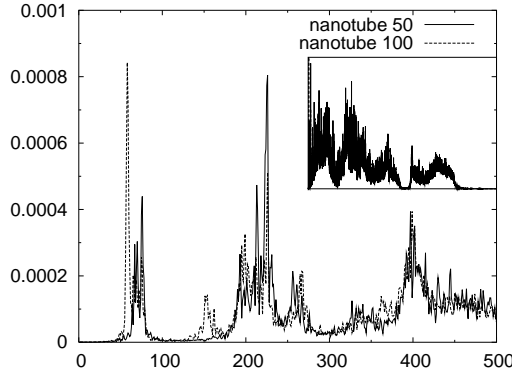


FIG. 6: Vibrational density of states of CNT $(10, 10)$ with 50 and 100 layers, respectively. Inset shows the VDOS in the full frequency range, and the full graph shows the VDOS in the low frequency range. In the graphs, dash lines denotes VDOS of CNT with 100 layers and solid line denotes VDOS of CNT with 50 layers.

## IV. CONCLUSIONS

In this paper the high thermal conductance of single-wall CNTs is calculated using equilibrium MD, and the relationship between thermal conductance and length of CNT is discussed. It is found that as a kind of quasi one dimensional material, CNT's thermal conductance doesn't converge to a finite value as the CNT length increases up to 80 nm. It can also be seen that longer CNT has more long wavelength vibrational modes, and these modes contribute to the thermal conduction as the CNT is longer.

----

[*] Electronic address: smayzh@nus.edu.sg

[†] also in Department of Computational Science, National University of Singapore, Singapore 117543

[1] S. Iijima, Naure **354**, 56 (1991).

[2] M. S. Dresslhaus, G. Dresselhaus, and R. Saito, Carbon **33**, 883 (1995); J. W. Mintmire and C. T. White, Carbon **33**, 893 (1995).

[3] Z. Yao, C.-C. Zhu, M. Cheng and J. Liu, Computational Material Science **22**, 180 (2001).

[4] S. Harris, *An Introduction to the Theory of the Boltzmann Equation* (Holt, Rinehart and Winston, New York, 1971); E. M. Lifshitz and L. .P. Pitaevskii, *Physical Kinetics* (Pergamon Press, Oxford, New York, 1981).

[5] R. Kubo, M. Toda, and N. Hashitsume, *Statistical Physics*, vol 2 (Berlin, Springer, 1985).

[6] S. Lepri, R. Livi, and A. Politi, Physics Reports **377**, 1 (2003).

[7] B. Li, *et al*, Phys. Rev. Lett. **88**, 223901 (2002); B. Li *et al*, Phys. Rev. E **67**, 021204 (2003); B. Li *et al*, cond-mat/0307692.

[8] J.-S. Wang, B. Li, cond-mat/0308445.

[9] B. T. Kelly, *Physics of Graphite* (Englewood Cliffs, NJL Applied Science, 1981).

[10] S. Maruyama, Physica B **323**, 193 (2002).

[11] S. Berber, Y.-K. Kwon, and D. Tománek, Phys. Rev. Lett. **84**, 4613 (2000).

[12] J. Che, T. Çağın, and W. A. Goddard III, Nanotechnology **11**, 65 (2000); J. Che, T.Çağın, W. Deng, and W. A. Goddard III, J. Chem. Phys. **113** 6888 (2000).

[13] M. A. Osman and D. Srivastava, Nanotechnology **12**, 21 (2001).

[14] S. G. Volz and G. Chen, Phys. Rev. B **61**, 2651 (2000); S. G. Volz and G. Chen, Appl. Phys. Lett. **75**, 2056(1999).

[15] D. Yang, Q. Zhang, G. Chen, S. F. Yoon, J. Ahn, *et al*, Phys. Rev. B **66**, 165440 (2002).

[16] P. Kim, L. Shi, A. Majumdar and P. L. McEuen, Phys. Rev. Lett. **87**, 215502 (2001).

[17] J. Hone, M. Whitney, C. Piskoti, and A. Zettl, Phys. Rev. B **59**, R2514 (1999).

[18] P. K. Schelling, S. R. Phillpot, and P. Keblinski, Phys. Rev. B **65**, 144306 (2002).

[19] A. J. C. Ladd, B. Moran, and W. G. Hoover, Phys. Rev. B **34**, 5058 (1986).

[20] J. Tersoff, Phys. Rev. B **39**, 5566 (1989).

[21] D. W. Brenner, Phys. Rev. B **42**, 9458 (1990).

[22] D. W. Brenner, O. A. Shenderova, J. A. Harrison, *et al*, J. Phys.: Cond. Matter **14**, 783 (2002).

[23] N. .A. Marks, Phys. Rev. B **63**, 035401 (2000).

[24] D. G. Pettifor and I. I. Oleinik, Phys. Rev. B **59**, 8487 (1999); D. G. Pettifor and I. I. Oleinik, Phys. Rev. B **59**, 8500 (1999).

[25] Q. Zheng, G. Su, J. Wang, and H. Guo, Eur. Phys. J. B **25**, 233 (2002).

[26] Z. Yao, J. -S. Wang, G. Liu, M. Cheng, physics/0311055.

[27] S. Nośe, Mol. Phys. **52**, 255 (1984); W. G. Hoover, Phys. Rev. A **31**, 1695 (1985).

[28] S. Muto and H. Aoki, J. Phys.: Cond. Matter **12**, L83 (2000).

[29] We run over $10^8$ steps, as a large number of steps is needed for obtaining accurate heat flux autocorrelation function data in our work.